Position Control of Belt-drive System Using Robust LQ Controller

M2014SC009 Toma KATO
supervisor : Isao TAKAMI

Abstract

In this study, a controller which has high applicability to the actual situation of industry is proposed by discussing about robust control of belt-drive system. First, the control target is represented by mathematical model. Second, the variation and uncertainty of the system are represented by polytope. Third, the controller which guarantees robust stability is designed by using LMI solution to the optimal regulator problem. Fourth, the robustness of the controller is verified by conducting simulation. Finally, experiment is conducted. In the experiment, the robustness and superiority of proposed method is established by comparing with a popular method.

1 Introduction

Power train means the mechanical device which conveys rotary power by using belt, chain, gear and so on. It is applied in many sectors of industry, for example, the timing belt of car engine, the belt conveyer of factory and so on. Therefore, to regulate the position or velocity conveyed by power train accurately is the exceedingly important problem for industrial application of the control method. However, in most cases of industrial application, the control target has some undesirable elements for designing the controller. For example, influence of disturbances, wear of parts, uncertain parameter and so on. Various methods for the motion control were proposed by researchers. For example, propotional-integral-derivative (PID) control is chosen in most industrial applications. However, it has vulnerability to the variation of system. Then, various methods for the robust stability were proposed. However, most of them are based on the complicated theory. Then, this study propose the method which has robustness, and designing that is comparatively easy.

2 Modeling

2.1 Control Target

The structure of the experimental device used in this study is shown in Fig. 1. Further, Table 1 shows physical constants and variables.

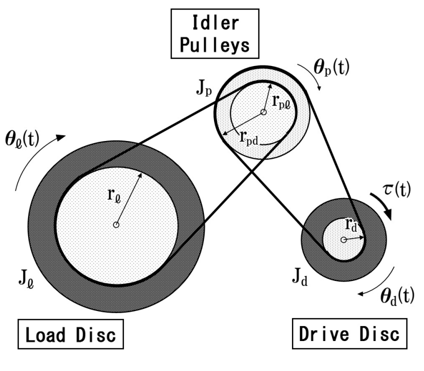

Figure 1 Structure of the Experimental Device

Table 1 Physical Constants and Variables

r_d	Radius of Drive Disc gear	[m]
r_{pd}	Radius of Idler Pulleys gear (connected to Drive Disc)	[m]
r_{pl}	Radius of Idler Pulleys gear (connected to Load Disc)	[m]
r_l	Radius of Load Disc gear	[m]
θ_d	Angle of Drive Disc	[rad]
θ_p	Angle of Idler Pulleys	[rad]
θ_l	Angle of Load Disc	[rad]
J_d	Inertia of Drive Disc	[kg·m^2]
J_p	Inertia of Idler Pulleys	[kg·m^2]
J_l	Inertia of Load Disc	[kg·m^2]
τ	Torque acting on Drive Disc	[Nm]
c_d	Friction coefficient of Drive Disc	[Nm/(rad/s)]
c_l	Friction coefficient of Load Disc	[Nm/(rad/s)]

It consists of three discs and two belts mainly. The discs are called Drive Disc, Idler Pulleys and Load Disc respectively. A motor connected to the Drive Disc gives input torque to the system. Then, the Idler Pulleys and the belts transmit the power to the Load Disc. By putting some weights on the Drive Disc and the Load Disc, their inertias J_d and J_l are changed. In other words, we can verify the effectiveness of a controller with various cases. The subject of this study is to control the Load Disc angle $\theta_l(t)$ by the input torque $\tau(t)$ acting on the Drive Disc.

2.2 Dynamical Equation

We treat three angles θ_d, θ_p and θ_l here. Let us derive three dynamical equations corresponding to each of the angles. First, let us focus on the Drive Disc.

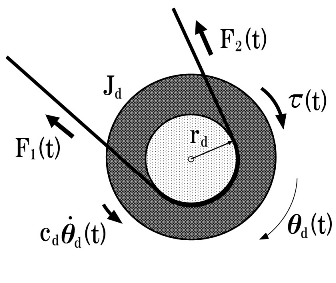

Figure 2 Enlarged Figure of the Drive Disc

Here, $F_1(t)$ and $F_2(t)$ are tension of the belt between the Drive Disc and the Idler Pulleys, and c_d is the friction coefficient of the Drive Disc. From Fig. 2, the dynamical equation of the Drive Disc is derived as Eq.(1).

$$J_d\ddot{\theta}_d(t) = \tau(t) + \{F_1(t) - F_2(t)\}r_d - c_d\dot{\theta}_d(t) \qquad (1)$$

Second, let us focus on the Idler Pulleys.

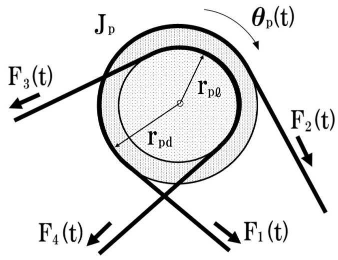

Figure 3 Enlarged Figure of the Idler Pulleys

Here, $F_3(t)$, $F_4(t)$ are tension of the belt between the Idler Pulleys and the Load Disc. From Fig. 3, the dynamical equation of the Idler Pulleys is derived as Eq.(2).

$$J_p\ddot{\theta}_p(t) = \{F_2(t) - F_1(t)\}r_{pd} + \{F_4(t) - F_3(t)\}r_{pl} \quad (2)$$

Finally, let us focus on the Load Disc.

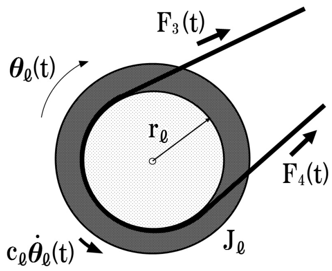

Figure 4 Enlarged Figure of the Load Disc

Here, c_l is the friction coefficient of the Load Disc. From Fig. 4, the dynamical equation of the Load Disc is derived as Eq.(3).

$$J_l\ddot{\theta}_l(t) = \{F_3(t) - F_4(t)\}r_l - c_l\dot{\theta}_l(t) \quad (3)$$

2.3 Spring Constant of the Belt

We obtain the following equation by transforming Eq.(2).

$$\{F_1(t) - F_2(t)\} = \frac{1}{r_{pd}}\left[\{F_4(t) - F_3(t)\}r_{pl} - J_p\ddot{\theta}_p(t)\right] \quad (4)$$

By substituting this equation into Eq.(1), we obtain the following equation.

$$\begin{aligned} J_d\ddot{\theta}_d(t) = \ & \tau(t) - c_d\dot{\theta}_d(t) \\ & + \frac{r_d}{r_{pd}}\left[\{F_4(t) - F_3(t)\}r_{pl} - J_p\ddot{\theta}_p(t)\right] \end{aligned} \quad (5)$$

By regarding the belt between the Idler Pulleys and Load Disc as the spring whose spring constant is k_{pl} as shown in Fig. 5, we obtain Eq.(6), (7). Here, F_0 is the initial tension of the belt.

$$F_3(t) = F_0 + k_{pl}\{r_{pl}\theta_p(t) - r_l\theta_l(t)\} \quad (6)$$

$$F_4(t) = F_0 - k_{pl}\{r_{pl}\theta_p(t) - r_l\theta_l(t)\} \quad (7)$$

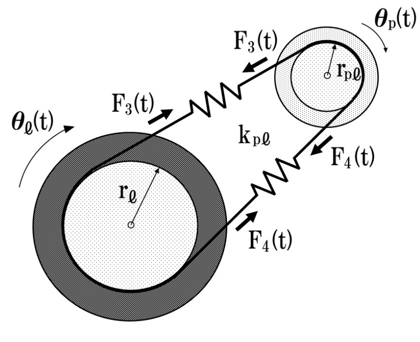

Figure 5 Belt between Idler Pulleys and Load Disc

The following equations are obtained by substituting Eq.(6), eq:F4 into Eq.(5), (3) respectively.

$$\begin{aligned} J_d\ddot{\theta}_d(t) = \ & \tau(t) - c_d\dot{\theta}_d(t) \\ & + \frac{r_d}{r_{pd}}\Big[-2k_{pl}\{r_{pl}\theta_p(t) - r_l\theta_l(t)\}r_{pl} \\ & - J_p\ddot{\theta}_p(t)\Big] \end{aligned} \quad (8)$$

$$J_l\ddot{\theta}_l(t) = 2k_{pl}\{r_{pl}\theta_p(t) - r_l\theta_l(t)\}r_l - c_l\dot{\theta}_l(t) \quad (9)$$

Now, let us define a constant k as follows for simplicity.

$$k \stackrel{\triangle}{=} 2k_{pl}r_l^2 \quad (10)$$

The following equations are obtained by applying k to Eq.(8) and Eq.(9).

$$\begin{aligned} J_d\ddot{\theta}_d(t) = \ & \tau(t) - c_d\dot{\theta}_d(t) \\ & + \frac{r_d}{r_{pd}}\left\{-\frac{r_{pl}^2}{r_l^2}k\theta_p(t) + \frac{r_{pl}}{r_l}k\theta_l(t) - J_p\ddot{\theta}_p(t)\right\} \end{aligned} \quad (11)$$

$$J_l\ddot{\theta}_l(t) = \frac{r_{pl}}{r_l}k\theta_p(t) - k\theta_l(t) - c_l\dot{\theta}_l(t) \quad (12)$$

2.4 Gear Ratio

Now let g_r' be the gear ratio of the Drive Disc and the Idler Pulleys as shown in Eq.(13). Furthermore, let g_r be the gear ratio of the Drive Disc and Load Disc as shown in Eq.(14).

$$g_r' \stackrel{\triangle}{=} \frac{r_{pd}}{r_d} \quad (13)$$

$$g_r \stackrel{\triangle}{=} g_r' \cdot \frac{r_l}{r_{pl}} \quad \left(= \frac{r_{pd}}{r_d} \cdot \frac{r_l}{r_{pl}}\right) \quad (14)$$

Then, the following equations hold as a fundamental property of the gear mechanism for power transmission.

$$\theta_d(t) = g_r'\theta_p(t),\ \dot{\theta}_d(t) = g_r'\dot{\theta}_p(t),\ \ddot{\theta}_d(t) = g_r'\ddot{\theta}_p(t) \quad (15)$$

$$\theta_d(t) = g_r\theta_l(t)\ ,\ \ \dot{\theta}_d(t) = g_r\dot{\theta}_l(t)\ ,\ \ \ddot{\theta}_d(t) = g_r\ddot{\theta}_l(t) \quad (16)$$

The following equations are obtained by applying g_r' and g_r to Eq.(11) and Eq.(12).

$$\begin{aligned} \tau(t) = & J_d\ddot{\theta}_d(t) + {g_r'}^{-2}J_p\ddot{\theta}_d(t) + c_d\dot{\theta}_d(t) \\ & + {g_r}^{-2}k\theta_d(t) - {g_r}^{-1}k\theta_l(t) \end{aligned} \quad (17)$$

$$0 = J_l\ddot{\theta}_l(t) + c_l\dot{\theta}_l(t) + k\theta_l(t) - {g_r}^{-1}k\theta_d(t) \quad (18)$$

Now let us define a constant J_d^* as follows.

$$J_d^* \triangleq J_d + {g_r}'^{-2} J_p \tag{19}$$

The following equation is obtained by applying J_d^* to Eq.(17).

$$\tau(t) = J_d^* \ddot{\theta}_d(t) + c_d \dot{\theta}_d(t) + {g_r}^{-2} k \theta_d(t) - {g_r}^{-1} k \theta_l(t) \tag{20}$$

2.5 State Space Representation

The following equations are obtained by representing Eq.(18) and Eq.(20) by matrices.

$$\boldsymbol{T} = \boldsymbol{D} \begin{bmatrix} \ddot{\theta}_d(t) \\ \ddot{\theta}_l(t) \end{bmatrix} + \boldsymbol{E} \begin{bmatrix} \dot{\theta}_d(t) \\ \dot{\theta}_l(t) \end{bmatrix} + \boldsymbol{F} \begin{bmatrix} \theta_d(t) \\ \theta_l(t) \end{bmatrix} \tag{21}$$

$$\boldsymbol{T} = \begin{bmatrix} \tau(t) \\ 0 \end{bmatrix} , \quad \boldsymbol{D} = \begin{bmatrix} J_d^* & 0 \\ 0 & J_l \end{bmatrix}$$

$$\boldsymbol{E} = \begin{bmatrix} c_d & 0 \\ 0 & c_l \end{bmatrix} , \quad \boldsymbol{F} = \begin{bmatrix} k{g_r}^{-2} & -k{g_r}^{-1} \\ -k{g_r}^{-1} & k \end{bmatrix}$$

The state space representation of the control target is obtained from Eq.(21) as follows.[1]

$$\begin{cases} \dot{x}(t) = Ax(t) + Bu(t) \\ y(t) = Cx(t) \end{cases} \tag{22}$$

$$A = \begin{bmatrix} 0 & 1 & 0 & 0 \\ -\frac{k{g_r}^{-2}}{J_d^*} & -\frac{c_d}{J_d^*} & \frac{k{g_r}^{-1}}{J_d^*} & 0 \\ 0 & 0 & 0 & 1 \\ \frac{k{g_r}^{-1}}{J_l} & 0 & -\frac{k}{J_l} & -\frac{c_l}{J_l} \end{bmatrix} \tag{23}$$

$$B = \begin{bmatrix} 0 \\ \frac{1}{J_d^*} \\ 0 \\ 0 \end{bmatrix} , \quad C = \begin{bmatrix} 0 & 0 & 1 & 0 \end{bmatrix} \tag{24}$$

$$x(t) = \begin{bmatrix} \theta_d(t) \\ \dot{\theta}_d(t) \\ \theta_l(t) \\ \dot{\theta}_l(t) \end{bmatrix} , \quad u(t) = \tau(t) \tag{25}$$

3 Control Design

In this section, we design a controller which guarantees robust stability to variation of the inertias J_d, J_l and uncertainty of the friction coefficients c_d, c_l.

3.1 Polytopic Representation

The ranges of the variation parameters J_d, J_l are as shown in Eq.(26), (27). On the other hand, let us define the range of the uncertain parameters c_d, c_l as Eq.(28), (29).

$$J_d^* \in [J_{d,min}^*, \ \ J_{d,max}^*] = [4.2 \times 10^{-4}, \ \ 5.5 \times 10^{-3}] \tag{26}$$

$$J_l \in [J_{l,min}, \ \ J_{l,max}] = [8.3 \times 10^{-3}, \ \ 2.8 \times 10^{-2}] \tag{27}$$

$$c_d \in [c_{d,min}, \ \ c_{d,max}] = [2.8 \times 10^{-3}, \ \ 5.7 \times 10^{-3}] \tag{28}$$

$$c_l \in [c_{l,min}, \ \ c_{l,max}] = [3.8 \times 10^{-2}, \ \ 6.8 \times 10^{-2}] \tag{29}$$

Then, Based on these ranges, let us define the vertexes of system matrices A and B as follows.

$$A_i \quad (i = 1, 2, 3, \cdots, 16) \quad , \quad B_i \quad (i = 1, 2, 3, \cdots, 16)$$

In Eq.(22), all of terms including the varying parameters J_d^*, J_l and uncertain parameters c_d, c_l are multi-affine for them. Therefore, if the stability at the vertexes shown in Eq.(30) is guaranteed, the robust stability to J_d^*, J_l, c_d and c_l is guaranteed among the ranges sown in Eq.(26) to (29).

3.2 LQ Optimal Control

Let us define $u(t)$ as the state feedback controller. Let Q be a weight matrix to state variable, and R a weight to input. Then, let us minimize the cost function J defined as following equation.

$$J = \int_0^\infty \{x(t)^T Q x(t) + u(t)^T R u(t)\} dt \tag{30}$$

Here, by using a feedback gain given as $K = YX^{-1}$, let us define $u(t) = Kx(t)$. Then, the system is stabilized by $u(t)$ if there exist X and Y satisfying following equations.[2]

$$\begin{bmatrix} He[A_i X + B_i Y] & X^T (Q^{\frac{1}{2}})^T & Y^T R \\ Q^{\frac{1}{2}} X & -I & O \\ RY & O & -R \end{bmatrix} \prec 0 \tag{31}$$

$$(i = 1, 2, 3, \cdots, 16)$$

$$\begin{bmatrix} Z & I \\ I & X \end{bmatrix} \succ 0 \quad , \qquad trace[Z] < \gamma \tag{32}$$

Here, X, Y are defined as $X \triangleq P^{-1}$, $Y \triangleq KX$. When we define the weights for state variable and input as Eq.(33), the feedback gain K is obtained as Eq.(34).

$$Q = \begin{bmatrix} 1 & 0 & 0 & 0 \\ 0 & 1 & 0 & 0 \\ 0 & 0 & 900 & 0 \\ 0 & 0 & 0 & 1 \end{bmatrix} \quad , \qquad R = 1800 \tag{33}$$

$$K_{opt} = \begin{bmatrix} -1.8324 & -0.1696 & 6.4070 & 0.4093 \end{bmatrix} \tag{34}$$

4 Simulation

In this section, the simulation is conducted with the proposed method. Here, the reference of the Load Disc angle $\theta_l(t)$ is $\frac{\pi}{2}$[rad]. By changing the condition of simulation model variously, the robustness of the controller is verified with various cases.[3] Table 2 shows conditions of the simulation.

Table 2 Simulation Conditions

	J_d^*	J_l	c_d	c_l
Nominal case	min	min	0.0043	0.053
Case 1	max	min	0.0043	0.053
Case 2	min	max	0.0043	0.053
Case 3	max	max	0.0043	0.053
Case 4	min	min	min	min
Case 5	min	min	max	max

Here, the "nominal case" assumes the state that Drive Disc and Load Disc have no weights, and the value of c_d, c_l is the middle point of their assumed range. The simulation results are shown by Fig. 6, 7.

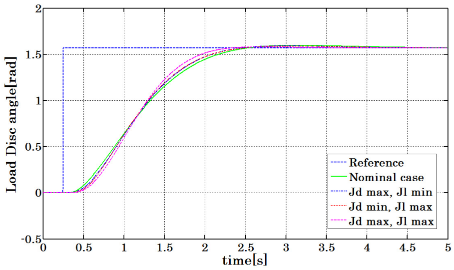

Figure 6 Simulation Result of Case 1 to 3

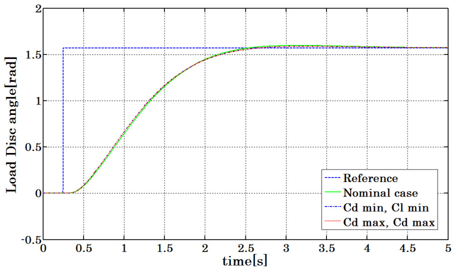

Figure 7 Simulation Result of Case 4, 5

This section shows the typical results, however that is not all. The simulation is conducted in all endpoints of the variation range which is defined as Eq.(26) to Eq.(29). Then, the controller makes Load Disc angle to follow the reference in all cases correctly. Thus the robustness of the controller is verified with simulation.

5 Experiment

By changing the set up of experimental device variously, the robustness of the controller is established with various cases. Furthermore, by comparing the propose method and nominal LQ, the superiority of the proposed method is proved. Table 3 shows conditions of the experiment.

Table 3 Experiment Conditions

	Drive Disc weight	Load Disc weight
Case 1	0	0
Case 2	4	0
Case 3	0	4
Case 4	2	2

The experiment results are shown by Fig. 8 to 11.

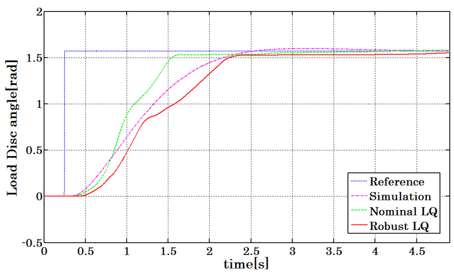

Figure 8 Experiment Result of Case 1

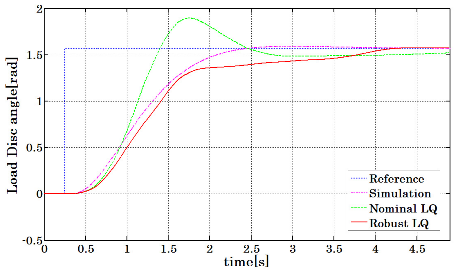

Figure 9 Experiment Result of Case 2

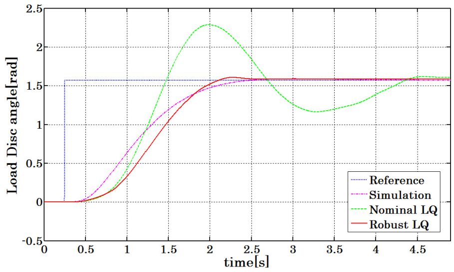

Figure 10 Experiment Result of Case 3

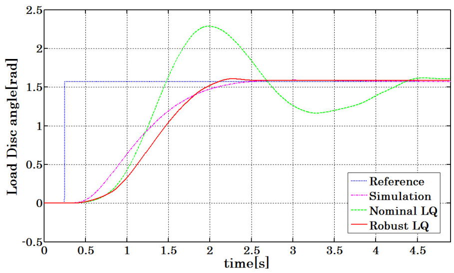

Figure 11 Experiment Result of Case 4

In some cases, the nominal LQ controller makes overshoot or oscillation. By contrast, the proposed method dose not make them in all cases. Thus the robustness and the superiority of the controller is established with the experiment.

6 Conclusion

In this study, robust LQ controller which guarantees robust stability to variation and uncertainty is designed by using polytopic representation and LMI solution to the optimal regulator problem. Further, the robustness and superiority of the proposed method is verified by simulation and experiment.

References

[1] Manual for Model 220 Industrial Emulator/Servo Trainer, Educational Control Products, 5725 Ostin Avenue, Woodland Hills, CA 91367, 1995.

[2] H.kataoka, T. Mizuno, H.Yamazaki, G.Chen, I. Takami: Robust Stabilization of Antilock Braking System with LQ Control. JSME, 2014, pp.1B24 1-11, 2014.

[3] Zhiqiang Gao, Shaohua Hu, and Fangjun Jiang: A Novel Motion Control Design Approach Based On Active Disturbance Rejection. Cleveland State University, Cleveland OH.